A Martin-Puplett Architecture for Polarization Modulation and Calibration

David T. Chuss[a], S. Harvey Moseley[a], Giles Novak[b], and Edward J. Wollack[a]

[a]NASA Goddard Space Flight Center, Code 685, Greenbelt, MD, USA;
[b]Northwestern University, Department of Physics and Astronomy, Evanston, IL, USA

ABSTRACT

We introduce an architecture for changing the polarization state of far-infrared through submillimeter radiation that employs two Martin-Puplett interferometers. One interferometer is oriented with its beam-splitting grid at an angle of 22.5° with respect to the Stokes Q axis. The second is oriented with its beam-splitting grid at an angle of 45°. By modulating one of the arms of each interferometer, it is possible to arbitrarily adjust the polarization state that a polarization-sensitive detector measures when placed at the output of the device. Because of this flexibility, one application of this device is as a calibrator for a polarimeter. In addition, it is conceivable to use such a device as a modulator for a far-infrared/submillimeter polarimeter. As such, this system has several advantages over a half-wave plate. First, the capability to measure circular polarization will provide the instrument with a novel method for checking systematic errors, as the circular polarization of most astronomical continuum sources is expected to be near zero. Second, such a device is easily adapted to work at different wavelengths, thus facilitating the construction of far-infrared and submillimeter polarimeters with multiple passbands. Finally, the small linear throws necessary for modulation eliminate the need for complicated systems of gears and low temperature bearings that are common in wave plate systems and often prone to failure. We present a Jones matrix analysis of this modulator architecture and compare the performance of this device with that of a half-wave plate.

Keywords: Polarization, Instrumentation, Modulation, Calibration

1. INTRODUCTION

The polarization state of light can be completely defined by the Stokes parameters Q, U, and V. (Stokes I is simply the total intensity of the radiation.) The set of all possible polarization states of light can be thought of as points in a three-dimensional space having Q, U, and V as coordinate axes. In such a space, a set of points sharing a common polarization,

$$P^2 = Q^2 + U^2 + V^2, \tag{1}$$

defines the surface of a sphere called the Poincaré sphere. The Poincaré sphere is a useful tool for studying polarization modulation that involves mapping between polarization states that have the same P. In this space, the action of an ideal modulator is a simple rotation.[1] Physically, a polarization modulation can be realized by introducing a phase delay between orthogonal polarization states. On the Poincaré sphere, orthogonal polarization states are those at opposite ends of a diameter. The geometrical effect of such a phase delay is a rotation about the diameter connecting the two orthogonal states. The magnitude of the rotation is equal to that of the phase delay.

Polarization modulation involves the transformation of one polarization state into a variety of others in a systematic way so as to enable the measurement of the initial state with a reduction of systematic errors. A convenient way of formulating the problem is to envision a detector that is sensitive to Stokes Q when projected onto the sky in the absence of modulation. The polarization modulator then transforms the polarization state to which the detector is sensitive.

Further author information: (Send correspondence to D.T.C.)
D.T.C.: E-mail: chuss@stars.gsfc.nasa.gov, Telephone: 1 301 286 1858

One method of polarization modulation involves the introduction of a phase delay between two orthogonal linear polarization states. If this phase delay is equal to π (a path difference of half of a wavelength), the effect is to reflect a linear polarization vector about the plane of symmetry of the device. If this phase is equal to one quarter of a wavelength, mapping between linear and circular polarization can occur.

The typical application of such a polarization modulator is a wave plate.[2] A wave plate consists of a piece of birefringent material cut so as to delay one polarization component relative to the other by the desired amount (generally either to one-half or one-quarter of the wavelength of interest). In this case, the phase difference is fixed and the modulation is accomplished by rotating the wave plate.

Conversely, it is possible to design a polarization modulator that holds the angle of the modulator fixed, but varies the phase. In this paper, we introduce a design for a polarization modulator that uses this strategy. This modulator consists of two Martin-Puplett interferometers[3] placed in series. Note that the Martin-Puplett interferometers discussed here do not include polarizing grids on the input or output stages of the device, as they often do in other applications. The first interferometer has its beam-splitting grid oriented at an angle of 22.5° with respect to the Stokes Q axis. By switching the phase difference the two polarizations between 0 and π, the output signal toggles between Q and U. Adding a second interferometer at an angle of 45° allows switching between either Q and $-Q$ or U and $-U$ depending on the state of the first interferometer.

There are several qualities that make this architecture a viable candidate technology for future astronomical polarimeters operating in the far-infrared through millimeter parts of the spectrum. First, whereas a given wave plate can be built to measure either circular or linear polarization but not both, the Martin-Puplett architecture's ability to cover the entire Poincaré sphere allows for the complete characterization of the polarization state. Second, since the path difference between orthogonal linear polarization states is variable, these devices are easily retuned for use at multiple wavelengths. Finally, this architecture requires only small linear translations that will eliminate the need for complicated systems of shafts and gears that are common in wave plate modulators. All of these qualities are beneficial to the future effort to measure the polarized flux of astronomical sources from space-borne telescopes.

2. JONES MATRIX FORMULATION

Jones matrices[4] are a convenient way to analyze radiation as it propagates through an optical system in situations such as those of interferometers where phase is important. In the following analysis, we use a formulation that is applicable for coherent radiation. In dealing with the general problem of partially coherent light, one can use the density matrix formulation[5]; however, for the following problem concerning polarization modulation, it is the coherent part of the formalism that is of interest. An additional caveat in the use of the Jones matrix formalism concerns its inability to handle reflections that cause backward traveling light in the optical path. However, in the Martin-Puplett architecture, the light never encounters a surface at normal incidence, and so this is not a concern for this analysis.

Jones Matrices are 2×2 matrices that contain information about how two orthogonal electric field components transform in an optical system. The input Jones vector is defined as follows:

$$|E\rangle = \begin{pmatrix} E_x \\ E_y \end{pmatrix} \equiv \begin{pmatrix} E_H \\ E_V \end{pmatrix} \tag{2}$$

The output vector from an optical system can then be represented by $|E_f\rangle = \bar{J}|E_i\rangle$ where $\bar{J}$ is the vector transformation introduced by the optical system. The power measured at a detector at the back end of such a system is given by $\langle E_f|\bar{J}_{det}|E_f\rangle = \langle E_i|\bar{J}^\dagger \bar{J}_{det}\bar{J}|E_i\rangle$. The matrix $\bar{J}_{det}$ is dependent on the properties of the detector used to make the measurement.

In the Jones matrix representation, Stokes parameters, which are particularly important in the study of polarization, are represented by the Pauli matrices and the identity matrix.

$$\bar{I} = \begin{pmatrix} 1 & 0 \\ 0 & 1 \end{pmatrix}, \bar{Q} = \begin{pmatrix} 1 & 0 \\ 0 & -1 \end{pmatrix}, \bar{U} = \begin{pmatrix} 0 & 1 \\ 1 & 0 \end{pmatrix}, \bar{V} = \begin{pmatrix} 0 & -i \\ i & 0 \end{pmatrix}, \tag{3}$$

Throughout this paper, we will use the convention that a bar over the Stokes symbol indicates its Jones matrix representation. An un-barred Stokes parameter represents power that can be measured (e.g. $Q = \langle E|\bar{Q}|E\rangle$).

These four Stokes matrices have the following multiplicative properties. Defining $(\bar{S}_0, \bar{S}_1, \bar{S}_2, \bar{S}_3) \equiv (\bar{I}, \bar{Q}, \bar{U}, \bar{V})$, $\bar{S}_0\bar{S}_\alpha = \bar{S}_\alpha\bar{S}_0 = \bar{S}_\alpha$ for $\alpha \in (0, 1, 2, 3)$ and $\bar{S}_j\bar{S}_k = \sum_l \epsilon_{jkl} i\bar{S}_l + \delta_{jk}\bar{S}_0$ for $j, k, l \in (1, 2, 3)$. These four matrices form a convenient basis for expressing Jones matrices. Table 1 Shows both the explicit Jones matrices and the Stokes expansion for selected optical transformations. The mirror transformation, which can be expressed simply as $\bar{Q}$, sets the convention for how the $(\hat{H}, \hat{V})$ coordinate system is propagated through the optical system. Note that for some structures, the Stokes expansion provides a convenient way to express optical elements. Successive transformations can be calculated either by matrix algebra or by the Pauli algebra defined above.

Table 1. A summary of physical transformation of optical elements, their Jones matrix representations, and their Pauli algebra representations are given.[6] For the linear distance transformation, d represents the distance traveled. For the mirror, a rotation of the mirror has no effect, and thus $\bar{Q}$ is a general representation for this element. For the wire grid, θ is the angle of the grid wires with respect to the $\hat{H}$-axis. For the rooftop mirror, θ is the angle between the roofline and the $\hat{H}$-axis. For the wave plate, θ is the angle between the fast axis of birefringence and the $\hat{H}$-axis, and ξ is half of the phase delay introduced between the orthogonal polarizations.

Description	Symbol	Matrix Representation	Stokes Expansion
Linear Distance	$\bar{J}_z(d)$	$\begin{pmatrix} \exp(i2\pi d/\lambda) & 0 \\ 0 & \exp(i2\pi d/\lambda) \end{pmatrix}$	$\bar{I}\exp(i2\pi d/\lambda)$
Mirror	$\bar{J}_M$	$\begin{pmatrix} 1 & 0 \\ 0 & -1 \end{pmatrix}$	$\bar{Q}$
Wire grid (ref.)	$\bar{J}_{WR}(\theta)$	$\begin{pmatrix} \cos^2\theta & \sin\theta\cos\theta \\ -\sin\theta\cos\theta & -\sin^2\theta \end{pmatrix}$	$\frac{1}{2}(\bar{Q} + \bar{I}\cos 2\theta + i\bar{V}\sin 2\theta)$
Wire grid (trans.)	$\bar{J}_{WT}(\theta)$	$\begin{pmatrix} \sin^2\theta & -\sin\theta\cos\theta \\ -\sin\theta\cos\theta & \cos^2\theta \end{pmatrix}$	$\frac{1}{2}(\bar{I} - \bar{Q}\cos 2\theta - \bar{U}\sin 2\theta)$
Coord. rotation	$\bar{R}(\theta)$	$\begin{pmatrix} \cos\theta & \sin\theta \\ -\sin\theta & \cos\theta \end{pmatrix}$	$\bar{I}\cos\theta + i\bar{V}\sin\theta$
Rooftop mirror	$\bar{J}_{RT}$	$\begin{pmatrix} \cos 2\theta & \sin 2\theta \\ \sin 2\theta & \cos 2\theta \end{pmatrix}$	$\bar{I}\cos 2\theta + i\bar{V}\sin 2\theta$
Wave plate	$\bar{J}_{WP}(\theta, \xi)$	$\begin{pmatrix} e^{i\xi}\cos^2\theta + e^{-i\xi}\sin^2\theta & \sin\theta\cos\theta(e^{i\xi} - e^{-i\xi}) \\ \sin\theta\cos\theta(e^{i\xi} - e^{-i\xi}) & e^{i\xi}\sin^2\theta + e^{-i\xi}\cos^2\theta \end{pmatrix}$	$\bar{I}\cos\xi + i\sin\xi(\bar{Q}\cos 2\theta + \bar{U}\sin 2\theta)$

2.1. Martin-Puplett Interferometer

A diagram of a Martin-Puplett Interferometer is shown in Figure 1. Light enters from the left and is split into two orthogonal polarizations by the 45° grid. The two components of polarization are then sent to two roof top mirrors which rotate the polarization by 90° with respect to the grid wires. The beams recombine at the beam splitter and exit the device at the top. Such a device is useful for retarding one polarization with respect to the other. This important property can be exploited to use this device as a polarization modulator.

We will examine this device using Jones matrices, defining the angle of the device to be the angle of the beam-splitting grid as seen by the incoming radiation. We will first look at the case of an interferometer at a rotation of 45° and then generalize to an arbitrary angle as was done above. For the simple case, the Jones matrix representing this configuration, $\bar{J}_{MP}(\pi/4)$, can be expressed as the sum of the Jones matrices for the radiation in each of the arms of the interferometer.

$$\bar{J}_{MP}\left(\frac{\pi}{4}\right) = \bar{J}^{(1)}_{MP}\left(\frac{\pi}{4}\right) + \bar{J}^{(2)}_{MP}\left(\frac{\pi}{4}\right) \tag{4}$$

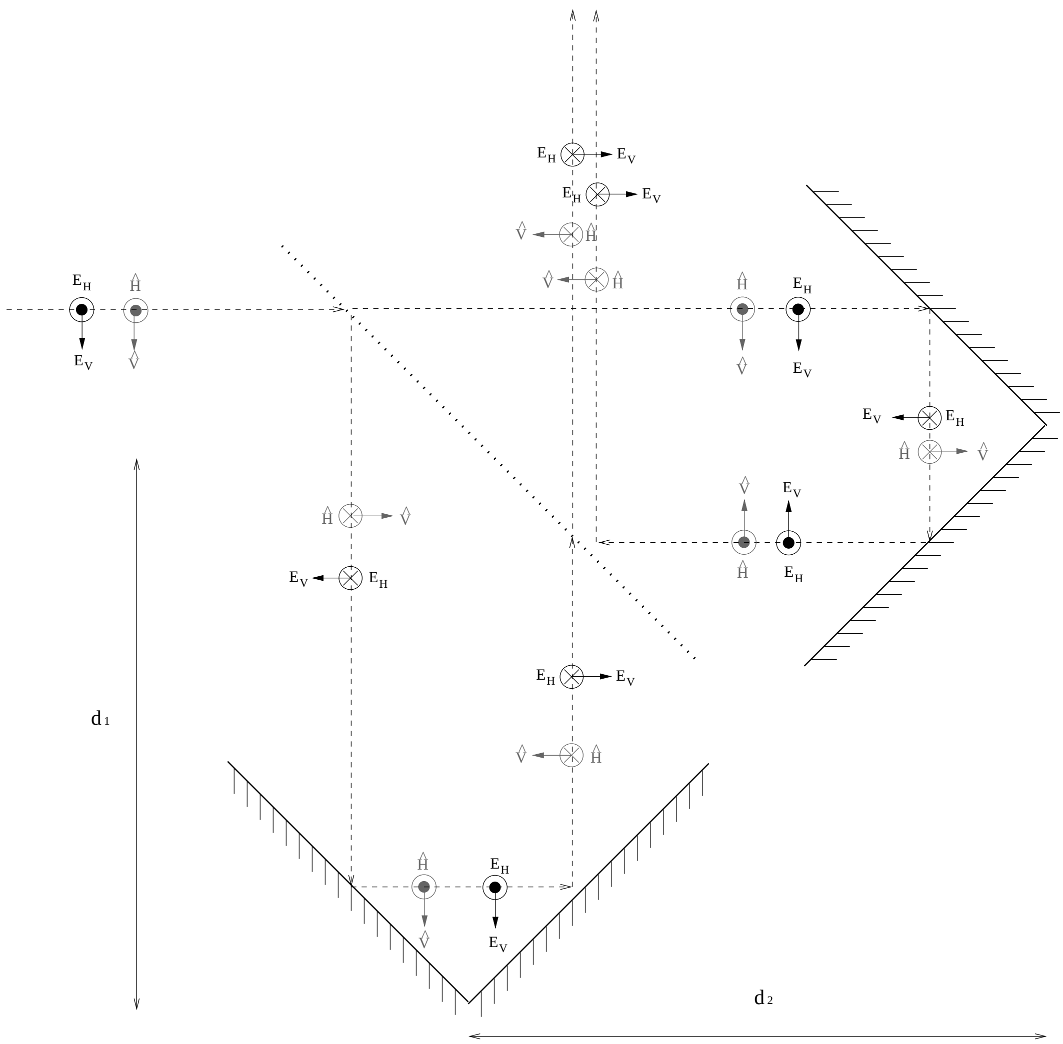

Figure 1. The propagation of the electric field components and the $(\hat{H}, \hat{V})$ coordinate axes through a Martin-Puplett interferometer at an angle of $\pi/4$ are shown. When $d_1 = d_2$, this device behaves like a mirror. When there is a path difference, it changes the polarization state of the incoming radiation.

In turn, each of these terms can be decomposed into a product of the Jones matrices of the individual elements in each optical path.

$$\bar{J}^{(1)}_{MP}\left(\frac{\pi}{4}\right) = \bar{J}_{WT}\left(\frac{\pi}{4}\right)\bar{J}_z(d_1)\bar{J}_{RT}(0)\bar{J}_z(d_1)\bar{J}_{WR}\left(\frac{\pi}{4}\right) = \begin{pmatrix} 1 & 1 \\ -1 & -1 \end{pmatrix}\frac{\exp(i4\pi d_1/\lambda)}{2}. \tag{5}$$

$$\bar{J}^{(2)}_{MP}\left(\frac{\pi}{4}\right) = \bar{J}_{WR}\left(-\frac{\pi}{4}\right)\bar{J}_z(d_2)\bar{J}_{RT}(0)\bar{J}_z(d_2)\bar{J}_{WT}\left(\frac{\pi}{4}\right) = \begin{pmatrix} 1 & -1 \\ 1 & -1 \end{pmatrix}\frac{\exp(i4\pi d_2/\lambda)}{2}. \tag{6}$$

Making the definition $\Delta \equiv 4\pi(d_2 - d_1)/\lambda$ and setting $d \equiv d_1$, we arrive at the following.

$$\bar{J}_{MP}\left(\frac{\pi}{4}\right) = \frac{1}{2}\mathrm{e}^{i4\pi d/\lambda}\begin{pmatrix} 1+\mathrm{e}^{i\Delta} & 1-\mathrm{e}^{i\Delta} \\ -1+\mathrm{e}^{i\Delta} & -1-\mathrm{e}^{i\Delta} \end{pmatrix} \tag{7}$$

Next, we derive an expression for a Martin-Puplett interferometer placed at an arbitrary angle θ. Recall that the definition of θ we have chosen is the angle of the grid with respect to $\hat{H}$ for the radiation at the input port. To do this, we transform into the coordinate system for which we have already solved the problem, apply the transformation for $\bar{J}_{MP}(\pi/4)$, and then transform back. In the case of the Martin-Puplett interferometer, there is a subtlety. Because the rooftop mirrors take the form of the identity matrix in one reference frame, they should function this way regardless of the orientation of the device. A consequence of this is that the correct transformation of this device is not achieved by rotating the individual elements. In short, the angular transformation matrix for this device should be the same as that for a grid. Setting $\chi = (\theta - \pi/4)$, we note that

$$\bar{J}_{MP}(\chi) = \bar{R}^{\dagger}(-\chi)\bar{J}_{MP}\left(\frac{\pi}{4}\right)\bar{R}(\chi) \tag{8}$$

$$\bar{J}_{MP}(\chi) = \frac{\mathrm{e}^{i4\pi d/\lambda}}{2}\begin{pmatrix} (1+\mathrm{e}^{i\Delta}) + (\mathrm{e}^{i\Delta}-1)\sin 2\chi & -(\mathrm{e}^{i\Delta}-1)\cos 2\chi \\ (\mathrm{e}^{i\Delta}-1)\cos 2\chi & -(\mathrm{e}^{i\Delta}+1) + (\mathrm{e}^{i\Delta}-1)\sin 2\chi \end{pmatrix} \tag{9}$$

$$\bar{J}_{MP}(\theta) = \mathrm{e}^{i4\pi d/\lambda}\left[\begin{pmatrix} 1 & 0 \\ 0 & -1 \end{pmatrix}\frac{1+\mathrm{e}^{i\Delta}}{2} + \begin{pmatrix} \cos 2\theta & \sin 2\theta \\ -\sin 2\theta & \cos 2\theta \end{pmatrix}\frac{1-\mathrm{e}^{i\Delta}}{2}\right] \tag{10}$$

$$\bar{J}_{MP}(\theta) = \mathrm{e}^{i4\pi d/\lambda}\left[\frac{1}{2}(1+\mathrm{e}^{i\Delta})\bar{Q} + \frac{1}{2}(1-\mathrm{e}^{i\Delta})\bar{R}(2\theta)\right] \tag{11}$$

When both arms of the interferometer are at equal distances ($\Delta = 0$), $\bar{J}_{MP}(\theta) = \bar{Q}\exp(i4\pi d/\lambda)$. Note that this is the same as a mirror reflection plus a linear distance. For a half-wave retardation, the first term in equation 10 drops out leaving only a pure rotation of the electric field vector. Finally, we wish to express the Martin-Puplett matrix as a linear combination of Stokes matrices. Thus, we obtain

$$\bar{J}_{MP}(\theta) = \mathrm{e}^{i2\pi(d_1+d_2)/\lambda}\left[\bar{Q}\cos\xi + i\sin\xi(\bar{I}\cos(2\theta) + i\bar{V}\sin(2\theta))\right] \tag{12}$$

Here, we have defined $\xi \equiv \Delta/2$ for notational convenience.

Note that within a phase factor (which is irrelevant in the final measurement) $\bar{J}_{MP} = \bar{Q}\bar{J}_{WP}$. This means that the action of the Martin-Puplett modulator is equivalent to that of a wave plate (a relative retardation between orthogonal linear polarization components) followed by a reflection (represented as the Jones matrix $\bar{Q}$).

2.2. Dual Modulators

We can write an expression for a modulator consisting of two Martin-Puplett interferometers having grid angles relative to the Stokes Q axis of θ_1 and θ_2. The corresponding phase delays are $\Delta_1 = 2\xi_1$ and $\Delta_2 = 2\xi_2$.

$$\bar{J}_m(\theta_1, \theta_2, \xi_1, \xi_2) \equiv \bar{J}_{MP}(\theta_1, \xi_1)\bar{J}_{MP}(\theta_2, \xi_2) \tag{13}$$

Note that the way we have configured the arrangement of interferometers, the light encounters the interferometer at θ_2 before the one at θ_1. Using Equation 12, we get the following.

$$\begin{aligned} \bar{J}_m(\theta_1, \theta_2, \xi_1, \xi_2) = \bar{I}\cos\xi_1\cos\xi_2 &+ [i\bar{Q}\cos 2\theta_2 + i\bar{U}\sin 2\theta_2]\cos\xi_1\sin\xi_2 \\ &+ [i\bar{Q}\cos 2\theta_1 - i\bar{U}\sin 2\theta_1]\cos\xi_2\sin\xi_1 \\ &- [\bar{I}\cos 2(\theta_1+\theta_2) + i\bar{V}\sin 2(\theta_1+\theta_2)]\sin\xi_1\sin\xi_2 \end{aligned} \tag{14}$$

This expression can be compared to that for dual wave plates where

$$\bar{J}_w(\theta_1, \theta_2, \xi_1, \xi_2) \equiv \bar{J}_{WP}(\theta_1, \xi_1)\bar{J}_{WP}(\theta_2, \xi_2) \tag{15}$$

In this case, we find

$$\begin{aligned} \bar{J}_w(\theta_1, \theta_2, \xi_1, \xi_2) = \bar{I}\cos\xi_1\cos\xi_2 &+ [i\bar{Q}\cos 2\theta_2 + i\bar{U}\sin 2\theta_2]\cos\xi_1\sin\xi_2 \\ &+ [i\bar{Q}\cos 2\theta_1 + i\bar{U}\sin 2\theta_1]\cos\xi_2\sin\xi_1 \\ &- [\bar{I}\cos 2(\theta_2-\theta_1) + i\bar{V}\sin 2(\theta_2-\theta_1)]\sin\xi_1\sin\xi_2 \end{aligned} \tag{16}$$

3. POLARIZATION MODULATION

3.1. The Single Modulator

In the following analysis, we assume that the detectors are sensitive to the difference between the power in two orthogonal linear polarization states. For ideal detectors, this leads to $\bar{J}_{det} = \bar{Q}$. It is thus the detector orientation that defines the coordinate axes from which the Stokes parameters are measured. For a single modulator, the signal at such a sensor is

$$\langle E_f|\bar{Q}|E_f\rangle = \langle E_i|\bar{J}^{\dagger}_{MP}(\theta,\Delta)\bar{Q}\bar{J}_{MP}(\theta,\Delta)|E_i\rangle. \tag{17}$$

Again, $\Delta = 2\xi$. Substituting Equation 12 into Equation 17 we find that the polarization signal one expects from a single Martin-Puplett modulator is

$$\langle E_f|\bar{Q}|E_f\rangle = Q\cos^2\xi + V\sin 2\theta\sin 2\xi + (Q\cos 4\theta + U\sin 4\theta)\sin^2\xi \tag{18}$$

We note that this is exactly the same function that describes a wave plate. The proof follows:

$$\bar{J}^{\dagger}_{MP}\bar{Q}\bar{J}_{MP} = (\bar{Q}\bar{J}_{WP})^{\dagger}\bar{Q}(\bar{Q}\bar{J}_{WP}) = \bar{J}^{\dagger}_{WP}\bar{Q}\bar{Q}\bar{Q}\bar{J}_{WP} = \bar{J}^{\dagger}_{WP}\bar{Q}\bar{J}_{WP} \tag{19}$$

For a single modulator (be it a wave plate or modulator) one can either modulate the angle of the relative retardation axis or the relative retardation itself. In practice, if one wishes to modulate the the angle, a wave plate is mechanically easier to rotate. Because the thickness of such a device is fixed, however, if one wishes to modulate the relative phase of the two polarizations, it is more convenient to use a Martin-Puplett architecture.

In wave plate applications, one typically holds $\xi = \pi/2$. For this case, we recover the result for a half-wave plate in which Q and U are modulated by $Q\cos 4\theta + U\cos 4\theta$. For a non-ideal half-wave plate, we find that with $\epsilon \equiv \frac{\Delta\lambda}{\lambda}\pi$, $\Delta = 2\xi = \pi + \epsilon$. To second order, this yields $\cos^2\xi = -\epsilon^2/2$, $\sin^2\xi = 1 - \epsilon^2/2$, and $\sin 2\xi = -\epsilon$. We find that at the edges of typical far-infrared/submillimeter passbands ($\frac{\Delta\lambda}{\lambda} \sim 0.1$), >90% of the total polarized power is still contained in the linear polarization modulation term with ∼10% being converted to V and $< 1\%$ appearing as the offset Q.

On the other hand, it is difficult to get efficient modulation with a single Martin-Puplett. Table 2 shows several attempts to fix the angle and modulate the phase. For the case in which the modulator is aligned with the detector's axis, no modulation occurs. For successively larger angles, some modulation occurs, but in no case are Q, U, and V completely modulated.

Table 2. The modulation of a single Martin-Puplett interferometer is described for four values of θ.

θ	Signal	Comment
0	Q	No Modulation
$\frac{\pi}{16}$	$Q\cos^2\xi + V\sin\frac{\pi}{8}\sin 2\xi + (Q+U)\frac{1}{\sqrt{2}}\sin^2\xi$	V completely modulated. Q and $(Q+U)$ cannot change sign.
$\frac{\pi}{8}$	$Q\cos^2\xi + U\sin^2\xi + \frac{V}{\sqrt{2}}\sin 2\xi$	V completely modulated. Q and U cannot change sign.
$\frac{\pi}{4}$	$Q\cos 2\xi + V\sin 2\xi$	Q and V completely modulated. U not measured.

3.2. The General Two-Element Modulator

Using a dual modulator gives additional degrees of freedom. For the Martin-Puplett architecture, this translates to the ability to modulate and measure Q, U, and V. For the wave-plate architecture, dual modulators allows for modulation over a broader frequency range.[7] The polarization signal for two Martin-Puplett modulators is

$$\langle E_f|\bar{Q}|E_f\rangle = \langle E_i|\bar{J}^{\dagger}_{m}(\theta_1,\theta_2,\Delta_1,\Delta_2)\bar{Q}\bar{J}_{m}(\theta_1,\theta_2,\Delta_1,\Delta_2)|E_i\rangle. \tag{20}$$

The calculation of the elements of $\bar{J}^{\dagger}_{m}(\theta_1,\theta_2,\Delta_1,\Delta_2)\bar{Q}\bar{J}_{m}(\theta_1,\theta_2,\Delta_1,\Delta_2)$ is given in Table 3 . The left hand column shows the factors that concern phase modulation, and the center and right hand column contains those that concern angle modulation. Each line of the table represents a term of the polarization signal that consists of the product of the factor in the left hand column and the corresponding angle factor.

Table 3. The functional form of the cases of dual Martin-Puplett interferometers and for dual wave plates.

Basis Function	Dual Martin-Puplett	Dual Wave Plate
$\frac{1}{4}(1+\cos\Delta_1)(1+\cos\Delta_2)$	Q	Q
$\frac{1}{4}(1+\cos\Delta_1)(1-\cos\Delta_2)$	$Q\cos 4\theta_2 + U\sin 4\theta_2$	$Q\cos 4\theta_2 + U\sin 4\theta_2$
$\frac{1}{4}(1-\cos\Delta_1)(1+\cos\Delta_2)$	$Q\cos 4\theta_1 - U\sin 4\theta_1$	$Q\cos 4\theta_1 + U\sin 4\theta_1$
$\frac{1}{4}(1-\cos\Delta_1)(1-\cos\Delta_2)$	$Q\cos 4(\theta_1+\theta_2) + U\sin 4(\theta_1+\theta_2)$	$Q\cos 4(\theta_2-\theta_1) - U\sin 4(\theta_2-\theta_1)$
$\frac{1}{2}(1+\cos\Delta_1)(\sin\Delta_2)$	$V\sin 2\theta_2$	$V\sin 2\theta_2$
$\frac{1}{2}(\sin\Delta_1)(1+\cos\Delta_2)$	$V\sin 2\theta_1$	$V\sin 2\theta_1$
$(\sin\Delta_1)(\sin\Delta_2)$	$\sin 2\theta_1\,(Q\sin 2\theta_2 - U\cos 2\theta_2)$	$\sin 2\theta_2\,(Q\sin 2\theta_1 + U\cos 2\theta_1)$
$\frac{1}{2}(\sin\Delta_1)(1-\cos\Delta_2)$	$V\sin 2\theta_1$	$-V\sin 2(2\theta_2-\theta_1)$
$\frac{1}{2}(1-\cos\Delta_1)(\sin\Delta_2)$	$V\sin 2(2\theta_1+\theta_2)$	$-V\sin 2\theta_2$

3.3. Dual Martin Puplett Interferometers- Fixed Angles

We look at the specific example of $\theta_1 = \pi/4$, $\theta_2 = \pi/8$. This corresponds to placing in the optical path one Martin-Puplett interferometer at an angle of $\pi/8$ followed by one oriented at angle of $\pi/4$. The functional form is given in Table 4 for $\bar{J}_m(\Delta_1, \Delta_2)$. This particular choice allows full modulation over the surface of the Poincaré sphere.

Table 4. The functional form of two stage Martin-Puplett polarization modulator is given. Here, we have fixed $\theta_1 = \pi/4$ and $\theta_2 = \pi/8$.

Basis Function	Coefficient
$\frac{1}{4}(1+\cos\Delta_1)(1+\cos\Delta_2)$	Q
$\frac{1}{4}(1+\cos\Delta_1)(1-\cos\Delta_2)$	U
$\frac{1}{4}(1-\cos\Delta_1)(1+\cos\Delta_2)$	$-Q$
$\frac{1}{4}(1-\cos\Delta_1)(1-\cos\Delta_2)$	$-U$
$\frac{1}{2}(1+\cos\Delta_1)(\sin\Delta_2)$	$\frac{1}{\sqrt{2}}V$
$\frac{1}{2}(\sin\Delta_1)(1+\cos\Delta_2)$	0
$(\sin\Delta_1)(\sin\Delta_2)$	$\frac{1}{\sqrt{2}}\,(Q-U)$
$\frac{1}{2}(\sin\Delta_1)(1-\cos\Delta_2)$	0
$\frac{1}{2}(1-\cos\Delta_1)(\sin\Delta_2)$	$-\frac{1}{\sqrt{2}}V$

4. MODULATION STRATEGY

For monochromatic radiation, modulation is simple. If we make the definition

$$\mathcal{A}(\Delta_1, \Delta_2) \equiv \langle E_i|\bar{J}_m^\dagger(\Delta_1, \Delta_2)\bar{Q}\bar{J}_m(\Delta_1, \Delta_2)|E_i\rangle, \tag{21}$$

the linear Stokes parameters are simply

$$Q = \frac{\mathcal{A}(0,0) - \mathcal{A}(\pi,0)}{2},\ U = \frac{\mathcal{A}(0,\pi) - \mathcal{A}(\pi,\pi)}{2}, V = \frac{\mathcal{A}(\pi/2,0) - \mathcal{A}(3\pi/2,0)}{2}. \tag{22}$$

For this simple modulation strategy, the bandwidth is plotted in Figure 2 along with a similar curve for a half-wave plate. The efficiency is determined by the fraction of the power that remains in linear polarization and is a function of wavelength. Note that for narrow bandwidths ($\Delta\lambda/\lambda \sim 0.1$), the performance of the dual

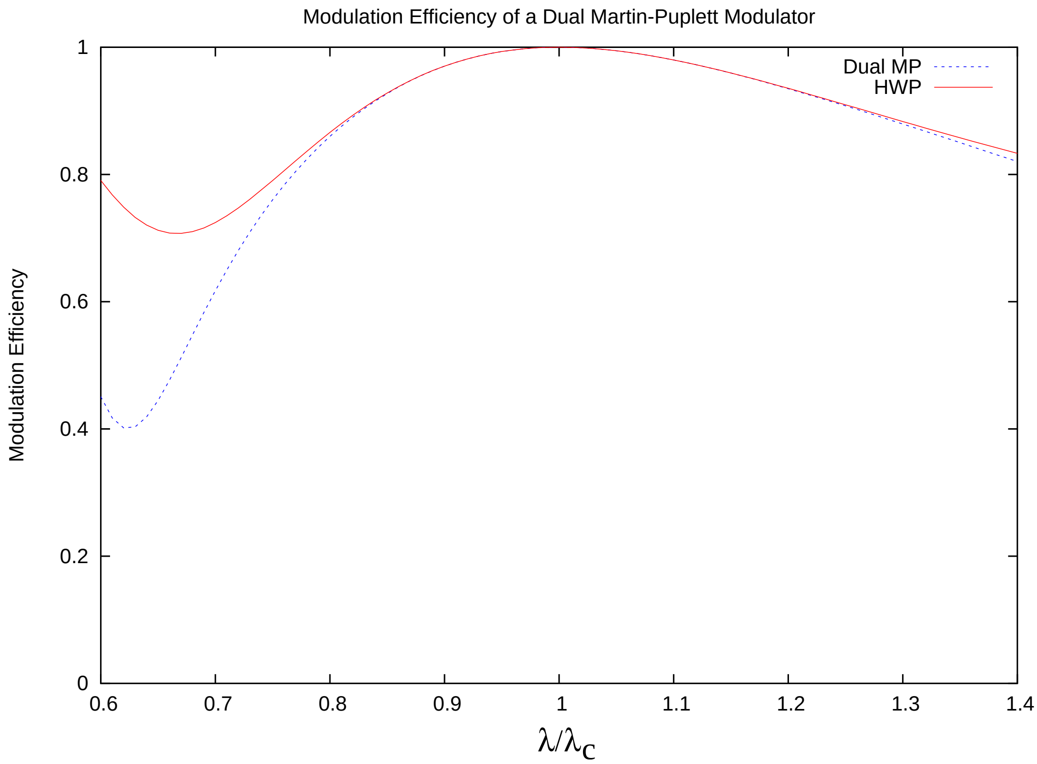

Figure 2. The bandwidth for a dual Martin-Puplett system is compared to that of a half-wave plate. The curves are calculated by transforming an input linear polarization signal by the action of the two devices and calculating the fraction of power remaining in the linear state ($\sqrt{Q^2+U^2}/\sqrt{Q^2+U^2+V^2}$).

Martin-Puplett interferometers matches the efficiency of a half-wave plate. Such bandwidths are common in far-infrared and submillimeter polarimetry.

This detection strategy is useful for systems having small $\Delta\lambda/\lambda$; however it suffers from a similar problem as a half-wave plate for wavelengths far from that for which the phase modulation has been optimized. In addition, systematics may be introduced by the fact that the error in $\mathcal{A}$ varies. The error introduced for $\mathcal{A}(0,0)$ will be zero; that introduced for $\mathcal{A}(\pi,\pi)$ will be maximal.

A more sophisticated technique for modulation takes advantage of the intrinsic broadband capabilities of this device. In reality, the electric field incident on the modulator can be decomposed into a linear combination of electric field vectors having a continuous distribution of wave numbers (k).

$$|\mathcal{E}_i\rangle = \int_0^\infty \psi(k)\mathrm{e}^{ik(z-ct)}|E_i(k)\rangle dk \tag{23}$$

Here, $\psi(k)$ is a function describing the bandpass of the instrument, and we have assumed propagation in the z-direction.

The signal at the detectors (using a differencing scheme) will be a function of k_1 and k_2, the wavenumbers corresponding to the delay in each of the two interferometers (i.e. $k_i = \pi/\delta d_i$, where δd_i is the physical path difference of the ith interferometer).

$$S(k_1,k_2) = \int_0^\infty \int_0^\infty \psi^*(k')\psi(k)\mathrm{e}^{i(k-k')(z-ct)} \langle E_i(k')|\bar{J}_m^\dagger(k')\bar{Q}\bar{J}_m(k)|E_i(k)\rangle dk' dk. \tag{24}$$

If $\psi(k)$ is a slowly varying function, the first integration over the exponential will only be non-zero for $k = k'$. This is equivalent to stating that the device is broadband. In this case, we have

$$S(k_1,k_2) = \int_0^\infty |\psi(k)|^2 \langle E_i(k)|\bar{J}_m^\dagger(k)\bar{Q}\bar{J}_m(k)|E_i(k)\rangle dk. \tag{25}$$

The operator $\bar{J}_m^\dagger(k')\bar{Q}\bar{J}_m(k)$ can be expressed in terms of a linear combination of Stokes parameters, the coefficients of which can be derived from the basis functions of Table 4. We then have

$$S(k_1,k_2) = \int_0^\infty |\psi(k)|^2 x_{k_1,k_2}(k) Q\, dk + \int_0^\infty |\psi(k)|^2 y_{k_1,k_2}(k) U\, dk + \int_0^\infty |\psi(k)|^2 z_{k_1,k_2}(k) V\, dk \tag{26}$$

$$x_{k_1,k_2}(k) = \left[1 + \cos\left(\frac{2\pi k}{k_2}\right)\right] \cos\left(\frac{2\pi k}{k_1}\right) + \sqrt{2}\sin\left(\frac{2\pi k}{k_1}\right)\sin\left(\frac{2\pi k}{k_2}\right)$$

$$y_{k_1,k_2}(k) = \left[1 - \cos\left(\frac{2\pi k}{k_2}\right)\right] \cos\left(\frac{2\pi k}{k_1}\right) - \sqrt{2}\sin\left(\frac{2\pi k}{k_1}\right)\sin\left(\frac{2\pi k}{k_2}\right)$$

$$z_{k_1,k_2}(k) = \frac{1}{\sqrt{2}}\sin\left(\frac{2\pi k}{k_2}\right)\cos\left(\frac{2\pi k}{k_1}\right)$$

Here, Q, U, and V are not barred to indicate that they are Stokes parameters and not their corresponding matrix representations. For most astrophysical applications of broadband polarimetry (i.e. polarization by dust emission, polarization of the CMB), it is assumed that the polarization does not change within the band. Put another way, what one measures in broadband polarimetry is the *average* Stokes parameters over a band. Each measurement then can be written in terms of these average Stokes parameters.

$$S(k_1,k_2) = \langle Q\rangle \int_0^\infty |\psi(k)|^2 x_{k_1,k_2}(k) dk + \langle U\rangle \int_0^\infty |\psi(k)|^2 y_{k_1,k_2}(k) dk + \langle V\rangle \int_0^\infty |\psi(k)|^2 z_{k_1,k_2}(k) dk \tag{27}$$

Here the bracketed quantities represent the Stokes parameters averaged over the band. If $|\psi(k)|^2$ is measured, these integrals can be calculated for various combinations of k_1 and k_2. A resulting fit can be done to determine the Stokes parameters for a given measurement.

5. IMPLEMENTATION

A possible practical implementation strategy for a modulator for an astronomical polarization is shown in Figure 3. In this realization, the retarding action of each Martin-Puplett interferometer is accomplished by two grids placed in front of two mirrors. Each grid/mirror pair accomplishes half of the desired retardation for each stage. The grids in front of a single rooftop mirror in this setup each have the same angle with respect to the optical coordinate system.

6. USE AS A CALIBRATOR

For experiments at long wavelengths such as those designed for measuring the polarization of the Cosmic Microwave Background (CMB), the long wavelengths and fast telescopes likely to be employed make dual Martin-Puplett interferometers difficult to employ. However, in the laboratory, the ability of these devices to work at room temperature may make them excellent calibrators. An input polarized signal can be transformed quite easily to test the polarization response of a CMB polarization sensor. It can transform an initial state that is linearly polarized into one that has most of its polarized power rotated into V. Using this technique, one can simulate the low linear polarizations of the CMB in the laboratory.

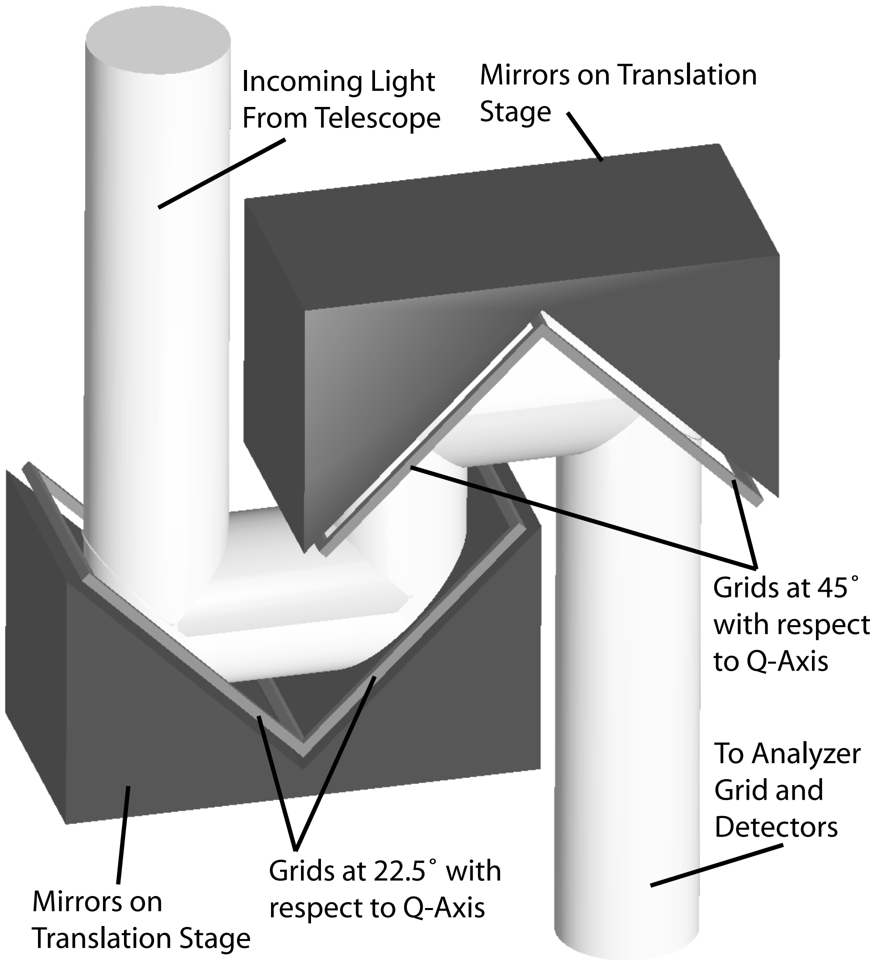

Figure 3. A variant of the dual Martin-Puplett polarization modulator is shown. Here, the action of each interferometer is divided between two grid-mirror pairs that form the two rooftop devices. In this case, the path length through the device is minimized. This helps minimize effects of changes in beam radius from one end of the modulator to the other when used in a real optical system. In addition, the proximity of the grids to the mirrors will allow for easier registration of the distances between them.[8] The geometry of the beam path is also favorable in this design in that the input and output beams are 180° apart. This allows for easier mechanical design.

7. SYSTEMATICS

In developing a polarization modulator, one must consider the possibility of instrumental effects introduced by the action of the modulation. In a half-wave plate, such an effect arises from the absorption properties of a birefringent dielectric. Loss tangents for light polarized along the fast and slow axis are generally different. The result is a modulated signal that appears at twice the rotational frequency of the wave plate. For the dual Martin-Puplett modulator, there are two important effects to consider. First, for different settings of the translational stage, the illumination will potentially change, thereby introducing a spurious polarization signal. This problem can be avoided by restricting the use of such modulators to slow optical systems in which the beam growth through the modulator is minimal. The second concern involves the differential absorption of the grids and the mirrors of the modulator. For the rooftop mirrors, the incident angle of the radiation is the same for different modulator positions. Thus, the Fresnel coefficients for each of the two polarizations will remain constant during the modulation process.

8. SUMMARY

We have described a new technique for polarization modulation and calibration applicable from the far-infrared through millimeter parts of the electromagnetic spectrum. In the far-infrared through submillimeter where bandpasses are typically $\Delta\lambda/\lambda \sim 0.1$, this device can be used in a similar manner to a half-wave plate. Broader bandpasses may be accommodated using more complex modulation schemes. In the millimeter, it may be useful as a calibrator for CMB missions.

The Martin-Puplett architecture provides a modulator that can be made robust, broadband, and easily tunable to different wavelengths. In addition, it allows for the complete determination of the polarization state of the incoming radiation by the measurement of Stokes Q, Stokes U, and Stokes V.

ACKNOWLEDGMENTS

We would like to thank Don Jennings for his helpful comments.

REFERENCES

1. J. Tinbergen, *Astronomical Polarimetry*, Cambridge, 1996.
2. R. H. Hildebrand, J. A. Davidson, J. L. Dotson, C. D. Dowell, G. Novak, and J. E. Vaillancourt, "A primer on far-infrared polarimetry," *PASP* **112**, pp. 1215–1235, 2000.
3. D. Martin and E. Puplett, "Polarised interferometric spectrometry for the millimetre and submillimetre spectrum," *Infrared Physics* **10**, pp. 105–109, 1970.
4. R. Jones, "New calculus for the treatment of optical systems," *J. Opt. Soc. Am.* **31**, pp. 488–493, 1941.
5. C. Brosseau, *Fundamentals of Polarized Light*, Wiley, 1998.
6. D. E. Budil, Z. Ding, G. R. Smith, and K. A. Earle, "Jones matrix formalism for quasioptical epr," *Journal of Magnetic Resonance* **144**, pp. 20–34, 2000.
7. S. Pancharatnam, "Achromatic combinations of birefringent plates," *Proc. Ind. Acad. Sci.* **41**, pp. 137–144, 1955.
8. T. Manabe, J. Inatani, A. Murk, R. J. Wylde, M. Seta, and D. H. Martin, "A new configuration of polarization-rotating dual-beam interferometer for space use," *IEEE Transactions on Microwave Theory and Techniques* **51**, pp. 1696–1704, June 2003.